Tracing the Assembly History of NGC 1395

Carlos G. Escudero[1,2,*], Favio R. Faifer[1,2], Analía V. Smith Castelli[1,2], Juan C. Forte[3,4], Leandro A. Sesto[1,2], Nélida M. Gonzalez[1,2], María C. Scalia[1,2]

1 Facultad de Ciencias Astronómicas y Geofísicas, UNLP
2 Instituto de Astrofísica de La Plata (IALP),CONICET-UNLP
3 Consejo Nacional de Investigaciones Científicas y Técnicas (CONICET)
4 Instituto Argentino de Matemática Alberto Calderón, CONICET

* Email: cgescudero@fcaglp.unlp.edu.ar

Facultad de Ciencias Astronómicas y Geofísicas UNIVERSIDAD NACIONAL DE LA PLATA

I A L P CONICET U N L P

Sistemas Estelares Extragalácticos y su Contexto Cosmológico

Introduction

In the scenario of galaxy formation, major fusions and tidal interactions play important roles. In the paradigm of hierarchical ΛCDM structure formation, **massive early-type galaxies** we see in the local Universe would have been **built through** a combination of **two phases**: in situ and ex situ formation (e.g., Oser et al. 2010). In the **first phase (z ≳ 2)**, there is **rapid in situ star formation** driven by the infall of cold gas flows (Naab et al. 2009), followed by a largely quiescent evolution. The **second phase (i.e. ex situ)** is dominated mainly by successive **accretion of smaller structures** (Zolotov et al. 2010; Wellons et al. 2016). These two mechanisms should leave their signatures on the dynamics, chemistry, and kinematics of the galaxies, both in their inner regions and in their halos. In this context, **globular clusters (GCs)** have proved to be important tools for examining the early stages of galaxy formation, and also to **trace major star forming episodes in a galaxy**.

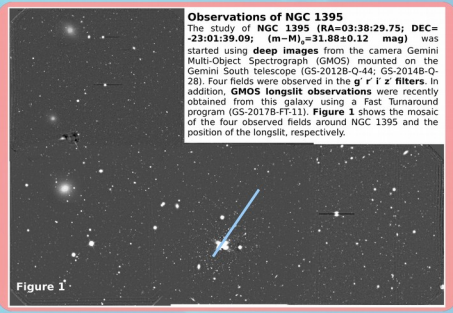

Figure 1

Observations of NGC 1395

The study of **NGC 1395 (RA=03:38:29.75; DEC=-23:01:39.09; $(m-M)_0$=31.88±0.12 mag)** was started using **deep images** from the camera Gemini Multi-Object Spectrograph (GMOS) mounted on the Gemini South telescope (GS-2012B-Q-44; GS-2014B-Q-28). Four fields were observed in the **g' r' i' z' filters**. In addition, **GMOS longslit observations** were recently obtained from this galaxy using a Fast Turnaround program (GS-2017B-FT-11). **Figure 1** shows the mosaic of the four observed fields around NGC 1395 and the position of the longslit, respectively.

Interaction Events in NGC 1395

Malin & Carter (1983) and Tal et al. (2009) mention that **NGC 1395** presents low contrast **shells** within its bright envelope. However, both papers do not present a characterization or description of them. We performed an analysis on our images with the aim at detecting some of these substructures. We used a combination of SExTRACTOR and the unsharp masking technique to detect and remove all the sources from the image, and also to highlight any possible remaining low surface brightness structure. **Figure 2** shows the location of a **faint shell** in the g' image at a galactocentric radius of **~3 arcmin (~20 kpc)** in the northwest direction. In addition, **a radial feature perpendicular to the shell is observed**, forming an umbrella-like structure (white arrows in Figure 2). This type of configuration likely created during the accretion of low-mass and gas-free galaxies on a nearly radial orbit, is frequently observed in early-type galaxies with stellar masses > $10^{10.1}$ M⊙ (Atkinson et al. 2013; Bilek et al. 2016). Since the dynamic age of these morphological disturbances seems to be ~0.5−3 Gyr (Pop et al. 2017), the presence of these substructures in NGC 1395 would indicate that **the galaxy has recently experienced, at least, one minor merger.**

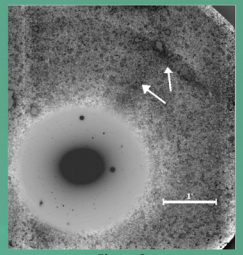

Figure 2

Globular Cluster System

Figure 3 shows the r_0 versus $(g'-z')_0$ diagram of the all unresolved sources detected in our GMOS mosaic. The selection of the **GC candidates of NGC 1395** was performed using different colour cuts (Escudero et al. 2018). The final GC candidates in our sample are displayed with black points. To investigate the different GC subpopulations present in NGC 1395, we used the Gaussian Mixture Modeling (GMM) code of Muratov & Gnedin (2010). The photometric analysis of the GC candidates reveals a **clear colour bimodality** distribution, indicating the presence of **"blue" (μ_b=0.93±0.01, σ_b=0.13±0.02 mag) and "red" (μ_r=1.33±0.02, σ_r=0.17±0.01 mag)** subpopulations (**Figure 4**).

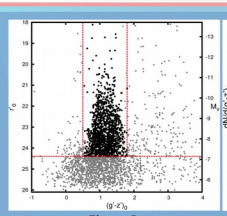

Figure 3

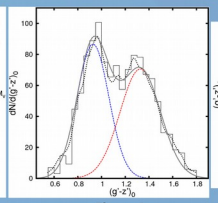

Figure 4

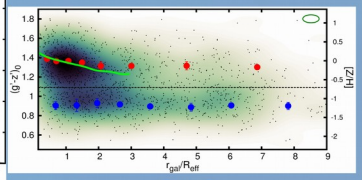

Figure 5

We obtained the mean colour of each subpopulation as a function of the normalized galactocentric radius (r_{gal}/R_{eff}), considering the **R_{eff}=1.07±0.03 arcmin (~7.1±0.2 kpc)**. We separated the GC sample in several galactocentric bins with the same number of objects, and we obtained the mean colour for each bin. **Figure 5** shows the **smoothed isocountor map of the GC radial colour distribution, the mean colours for each subpopulation, and the colour profile of the galaxy** (green solid line). The **red mean colours** in each radial bin reveal a colour **gradient**. We quantify these gradients obtaining **Δ[Z/H]/log(r_{gal}/R_{eff})=−0.09±0.07** dex per dex for the **blue**, and **Δ[Z/H]/log(r_{gal}/R_{eff})=−0.21±0.03** dex per dex for the **red** ones. The presence of these colour (metallicity) gradients, mainly evidenced by the red GC subpopulation within ~2R_{eff} (~14 kpc), suggest a **two-phase assembly for both clusters families** and, therefore, for NGC 1395. The figure also shows that the inner colour of **the halo of the galaxy** is in good agreement with the average colour of the **red clusters**. This similarity suggests a strong link between them, indicating **a likely joint stellar formation**. The absence of a significant metallicity gradient in the **blue GC subpopulation** suggests that this family would be comprised of a **strong mixing of blue clusters formed in situ in the galaxy and accreted from different satellite galaxies** (Harris et al. 2016).

Spatial Distribution

Figure 6 shows the **projected spatial distribution** through smoothed density maps of the **blue and red GC candidates** of NGC 1395 (top and bottom panels, respectively). Both families fill the entire GMOS mosaic, showing the **typical spatial distribution** found in early-type galaxies (Faifer et al. 2011; Escudero et al. 2015), with the red clusters more concentrated toward the galactic center in comparison with the blue ones. In addition to the different degree of concentration shown by both families, it is observed what seems to be a **mild overdensity** of objects (**r_{gal} < 1.6 arcmin; ~10 kpc**, white dashed circle) slightly offset from the galactic center, in a northwest direction **towards the shell location** (black strip). D'Abrusco et al. (2015) suggest that this type of overdensities may be driven by accretion of satellite galaxies, major dissipationless mergers, or wet dissipation mergers.

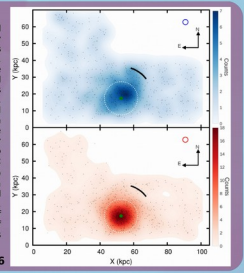

Figure 6

Stellar Population Analysis

As mentioned earlier, **NGC 1395** shows evidence of having experienced, **at least, one recent merger** event. Although some works in the literature have presented an analysis of the stellar population of the central region of NGC 1395, the values of age and metallicity obtained present slight differences. Therefore, recently, we obtained **GMOS longslit data** of the galaxy in order to derive accurate stellar population parameters. We determined the stellar population parameters of the galaxy using two methods: **Lick indices** with the simple stellar population (SSP) models of Thomas et al. (2003,2004), and **full spectral fitting** technique with UlySS (Koleva et al. 2009) code over a SSP basis from the PegaseHR models (Le Borgne et al. 2004). Both methods indicate that the **innermost region presents an intermediate age** (**Figure 7**), becoming older at higher galactocentric radii. On the other hand, the value of [α/Fe] remains constant, while a clear **metallicity gradient** is observed as well as in the photometric analysis.

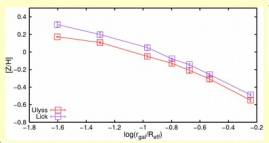

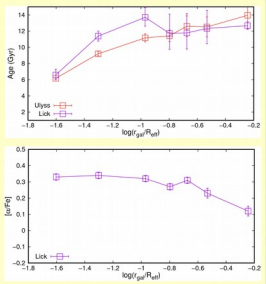

Figure 7

Summary and Conclusions

Using excellent Gemini/GMOS photometric and spectroscopic data, we studied the GC system of the elliptical galaxy NGC 1395, and also we determined the stellar population parameters. We detected the presence of a **faint inner shell** located at a galactocentric radius of ~3 arcmin (~20 kpc) in the northwest direction, **connected with a "radial feature"** forming an umbrella-like structure. The analysis of the **GC colour distribution** exhibits a **bimodal** appearance in the colours $(g'-z')_0$, indicating the presence of at least two GC subpopulations: the typical **blue (metal-poor) and red (metal-rich)** subpopulations. In particular, the **red subpopulation** presents a steep colour **(metallicity) gradient** (< 2R_{eff}; ~14 kpc) as a function of galactocentric radius compared to the **blue** one, with the latter exhibiting relatively **shallow metallicity gradients** throughout the system.These radial metallicity trends within ~2R_{eff}, and the subsequently flattening towards larger radii, would indicate that the **inner populations of the galaxy** (i.e. stars and GCs) have been formed by **in situ dissipative processes**. In addition, the observed similarity between the inner colour of the **halo of the galaxy** and the average colour of the **red subpopulation** would indicate a likely **joint stellar formation**, reinforcing the scenario previously mentioned. On the other hand, the absence of a significant colour (metallicity) gradient in the blue candidates suggests a growth of the outer halo due to continuous accretion of low mass systems with its GCs. Particularly, in this last point, the presence of a mild GC overdensity, mainly of blue candidates, is observed in the same direction as the shell structure. We determined the stellar population parameters at different galactocentric radii of NGC 1395, where a **clear metallicity gradient** was obtained.

Combining all the results obtained in this work, we have found that **the assembly of the elliptical galaxy NGC 1395**, and consequently the formation of its GC system, **would fit in the scenario of growth in "two-phases" or "inside-out"**. In this picture, the old age (r_{gal}>3 arcsec), steep metallicity gradients, and [α/Fe]~0.3 dex displayed by the galaxy, would indicate that the core of NGC 1395 had a rapid formation timescale, possibly dominated by in situ dissipative processes that formed the vast bulk of star and GCs. Subsequently, the continuos accretion of stars and mainly blue GCs belonging to low-mass satellite galaxies, have been increasing the mass growth of the galaxy, contributing to the metallicity gradient flattening. In addition, the presence of tidal structures indicates that the galaxy is still accreting group members.

References

Atkinson A. M., et al., 2013, ApJ, 765, 28
Bilek M., et al., 2016, A&A, 588, A77
D'Abrusco R., Fabbiano G., Zezas A., 2015, ApJ, 805, 26
Escudero C. G., et al., 2015, MNRAS, 449, 612
Escudero C. G., et al. 2018, MNRAS, 474, 4302
Faifer F. R., et al., 2011, MNRAS, 416, 155
Harris W. E., et al., 2016, ApJ, 817, 58
Koleva, M., et al., 2009, A&A, 501, 1269
Le Borgne, D., et al., 2004, A&A, 425, 881
Malin D. F., Carter D., 1983, ApJ, 274, 534
Muratov A. L., Gnedin O. Y., 2010, ApJ, 718, 1266
Naab T., et al., 2009, ApJ, 699, L178
Oser L., et al., 2010, ApJ, 725, 2312
Pop A., et al., 2017, arXiv:1706.06102
Tal T., et al., 2009, AJ, 138, 1417
Thomas D., et al., 2003, MNRAS, 339, 897
Thomas D., et al., 2004, MNRAS, 351, L19
Wellons S., et al., 2016, MNRAS, 456, 1030
Zolotov A., et al., 2010, ApJ, 721, 738

The Globular Cluster System of NGC 1395: combining optical and near infrared photometry

Faifer F.[1,2], Escudero C.[1,2], Smith Castelli A.[1,2], Sesto L.[1,2], Forte J. C.[3,4], Chies Santos A.[5], Cortesi A.[6], Mendes de Oliveira C.[6]

1: Facultad de Cs. Astr. Y Geof. UNLP (Argentina)
2: Instituto de Astrofísica de La Plata, UNLP-CONICET (Argentina)
3: CONICET (Argentina)
4: Instituto de Matematicas Juan Calderón, CONICET (Argentina)
5: Departamento de Astronomia, Instituto de Física, UFRGS (Brasil)
6: Departamento de Astronomia, IAG, Universidade de São Paulo (Brasil)

Introduction: In the framework of our BAGGs collaboration, we are involved in obtaining deep optical and NIR photometry, as well as deep MOS spectroscopy, of GC systems belonging to massive early-type galaxies. Combined with different SSP models, these data will help to mitigate the age-metallicity degeneracy and will allow us to measure several color-indices less sensitive to the effect of horizontal-branch stars. By combining kinematics and color-metallicity measurements of GC systems in a self-consistent manner, we recover the evolutionary histories of the galaxies and shed light in the assembly history of the halos of the galaxies. As a firts step of BAGGs' observing campaign, we observed the GC system of the giant elliptical galaxy NGC 1395 (D~21.4 Mpc, M_B=-21.02 mag), one of the dominant galaxies of the Eridanus group.This galaxy harbours thousands of GCs and show different GCs subpopulations in their optical color distributions (Escudero+ 2018). Here we are presenting our first results, based on deep and high quality NIR photometric data in two different photometric bands (J and Ks) obtained with GEMINI+Flamingos2 instrument which were combined with high quality optical photometry from previous GEMINI+GMOS runs.

Optical Data: We worked on images in the g' (4x180.5 seg), r' (4x120.5 seg), i' (4x150.5 seg) and z' (4x150.5 seg) bands obtained with GEMINI+GMOS (Programs GS-2012B-Q-44 and GS-2014B-Q-28) using binning 2x2 which gives a scale of 0.146"/pix. These images correspond to four science fields in the region of the elliptical galaxy NGC 1395, plus an additional comparison field. In this poster we present the results obtained from two fields. The complete optical photometric analysis is presented in Escudero+ (2018).

NIR Data: Within the BAGGs collaboration, we also obtained NIR images of two of the optical fields through GEMINI+Flamingos2 in the J and Ks bands (Program GS-2015B-Q-38). The exposure times were 30x50 seg on source + 18x50 seg on sky in both fields for the J band, and, in the Ks band, 302x12 seg on source + 120x12 seg on sky for the field containing the galaxy and 277x12 seg on source + 110x12 on sky for the other field. The NIR photometry was calibrated using 2MASS objects present in our fields.

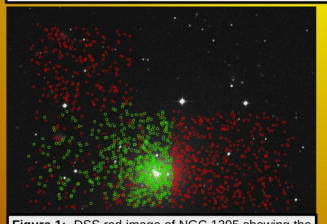

Figure 1: DSS red image of NGC 1395 showing the ~1300 optical GC candidates (red squares). The candidates (~520) detected in the J and Ks images are shown in green. The size of this mosaic is 12x17 arcmin. North is up and east to the left.

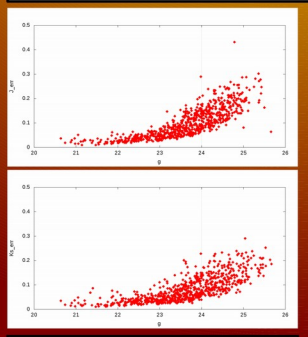

Figure 2: Photometric errors of the Daophot photometry in the J (upper panel) and Ks (lower panel) bands. The mean error for objects with g'<24 mag is 0.1 mag.

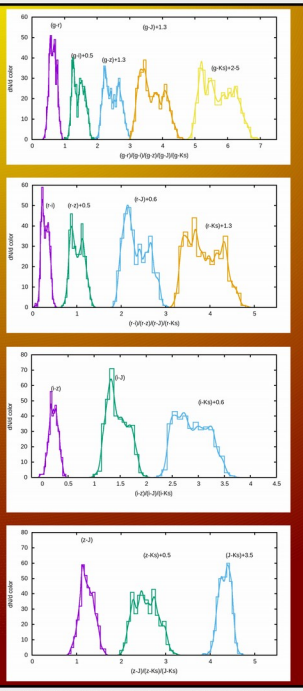

Figure 3: Histograms and density color distribution for different band combinations and for objects with g'<24 mag. The considered bins are in the range 0.04-0.1 mag. The density distribution was built using Gaussian kernels with σ in the range 0.02-0.05 mag. To avoid superposition, we shifted some histograms in a constant value indicated in the figures.

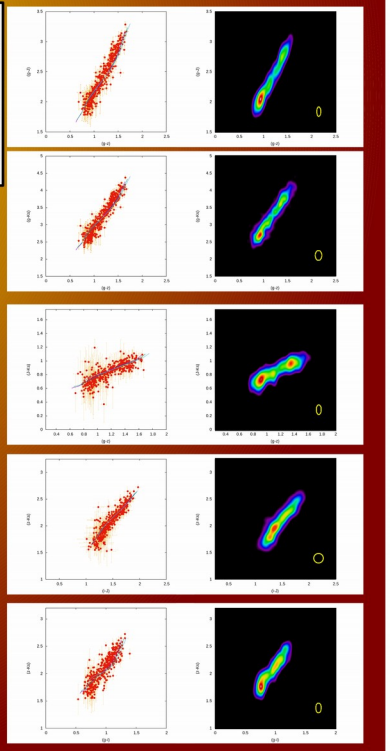

Figure 4: Color-color diagrams of our optical and NIR photometric sample are shown in left panels. The plots include ~360 objects with g'<24 mag, detected and successfully measured in g',r',i',z',J and Ks bands. The lines show the Yonsei Evolutionary Population Synthesis models (YEPS) for 8, 10 and 12 Gyr (violet, green and cyan lines, respectively). In order to match the photometry and the SSP models, an -0.15 and -0.27 mag offsets were applied to modeled J and Ks magnitudes. In the right panels we show density graphics of the same diagrams. The yellow circular/elliptical symbols depict the kernel used in each case.

Conclusions: The appearance of the color distribution strongly depends on which bands are combined. All the opical, optical-NIR and most of the purely NIR color distributions show evidence of the presence of multi-subpopulations. Some of them, like (r'-i'), (r'-z'), (g'-i'), (g'-z') and (g'-Ks), look strongly bimodal with possible substructures. As previously noticed by others authors (e.g. Cho+ 2016), in the particular case of colors involving only NIR bands, the situation is not so clear. However, thanks to our deep and clean photometry, it is possible to detect different kinds of substructures in all of them. YEPS models (Chung+ 2013) show a nice agreement with our observations.

The color-color diagrams show signs of different degrees of non-linearity. This is in good agreement with previous studies (Blakeslee+ 2012; Forte+ 2013; Cantiello+ 2014, Powalka+ 2016). Interestingly, most of the smoothed diagrams suggest that at least two main subpopulations in color are present. The combination (z'-Ks) vs (g'-i') resulted to be one of the most clearly non-linear cases. It is possible to see a "break" similar to that suspected in the (H-i') vs (g'-z') diagram of Cantiello+ (2014). This break produces a clear intermediate peak in the (z'-Ks) color distribution.